D15

WAKE CURVATURE AND TRAILING EDGE INTERACTION EFFECTS IN VISCOUS FLOW OVER AIRFOILS*

R.E. Melnik
Grumman Aerospace Corporation

SUMMARY

This paper describes a new theory developed by the author and his colleagues for analyzing viscous flows over airfoils at high Reynolds numbers. The theory includes a complete treatment of viscous interaction effects induced by the curved wake behind the airfoil and accounts for normal pressure gradients across the boundary layer in the trailing edge region. A brief description of a computer code that was developed to solve the extended viscous interaction equations is given. Comparisons of the theoretical results with wind tunnel data for two rear loaded airfoils at supercritical conditions are presented.

INTRODUCTION

Two classes of theoretical methods are currently employed in the analysis of viscous flows over airfoils; one based on a direct numerical solution of the Reynolds-averaged equations of turbulent flow (e.g., refs. 1 and 2) and the other on an approximate boundary layer type formulation. Because of the magnitude of the computational task direct solutions of the Reynolds equations have been restricted to relatively crude grids. Because of the long computing times and poor resolution, these methods are not yet suitable for practical applications. Most existing methods of analyzing the problem are based on the displacement surface concepts of conventional boundary layer theory (e.g., see ref. 3). Unfortunately these approaches themselves are not entirely satisfactory because they neglect certain strong interaction effects that occur near trailing edges and shock impingement zones. In addition, most of the boundary layer formulations employed in the past were incomplete in that they ignored certain effects due to the wake. These effects are formally the same order of magnitude (as a function of the Reynolds number, R_e for $R_e \to \infty$) as the usual displacement effects on the airfoil surface and should be included in a completely consistent theory.

There are two wake effects, one due to its thickness and the other to its curvature. The wake thickness effect leads to a semi-infinite equivalent displacement body that enters into the determinaton of the outer inviscid solution. Although there are no conceptual difficulties in doing this, the wake thickness terms have usually been dropped or drastically approximated (e.g., ref. 3) in most previous studies in the interest of simplifying the computations. The wake curvature effect arises from the turning of the low momentum flow in the wake along the curved streamlines behind the airfoil.

*This work was partially supported by NASA under Contract NAS 1-12426.

254

PAGE INTENTIONALLY BLANK

A consistent application of the method of matched asymptotic expansions (for $R_e \to \infty$) leads to a matching condition requiring a discontinuity of the pressure across the trailing streamline of the outer inviscid flow. This leads to an effect similar to a jet flap with a negative jet momentum coefficient and hence, to a reduction of the lift coefficient. Although the need to include the wake curvature terms has been recognized in the past (refs. 4-6) it was only recently (ref. 7) that a completely consistent computation including the wake has been carried out.

It is well known that the boundary layer approximations break down in shock wave boundary-layer interaction zones (see ref. 8). The present author and R. Chow has shown (ref. 9) that the boundary layer approximations also fail in interaction regions near trailing edges. Analysis of the higher-order terms indicates that normal pressure gradients are important across the boundary layer and must be included in a correct lowest-order description of the flow in these regions.

The present author and R. Chow have developed a complete theory for the inner region near cusped trailing edges. We also developed a simple procedure for using the local trailing edge solution to correct the conventional boundary layer formulation (ref. 7). The resulting theory correctly treats the wake and the strong interaction region near trailing edges. Both effects are potentially important because they directly influence the Kutta condition and can therefore have a large global effect on the lift, drag, and moment of the airfoil section.

In the present paper we briefly describe the new viscous theory including a description of the numerical methods employed to solve the resulting interaction equations. Typical theoretical results are compared with wind tunnel data on rear loaded airfoils and some conclusions are drawn regarding the practical importance of wake curvature effects.

In the present work we do not provide for a rational analysis of the shock wave boundary interaction problem arising in supercritical cases. Instead a local numerical smoothing of the boundary layer and inviscid solutions near shock impingement points is employed that enables the viscous theory to function in these cases. Experience has indicated that the smoothing only affects the local pressure distribution near the shock wave and does not greatly influence the predicted section characteristics of the airfoil. Although the new theory is strictly applicable only to cusped airfoils, a computer code was written that is applicable to more general airfoils with nonzero trailing edge angles. Results obtained to date indicate that the theory provides useful results for these more general airfoil sections.

BOUNDARY LAYER FORMULATION

In this section we review the matching conditions that couple the viscid and inviscid flow solutions in the conventional boundary layer formulation. The structure of the flow field at high Reynolds number is sketched in figure 1. There are several regions consisting of the outer inviscid flow,

thin shear layers on the airfoil, and in the wake and strong interaction regions near the trailing edge and shock impingement points. The conventional boundary layer formulation leads to matching conditions coupling the inviscid flow to the thin shear layers outside the strong interaction regions. There are several equivalent statements of the matching conditions (see ref. 10) that follow directly from the fact that the flow in the shear layers is governed by the boundary layer equations. The matching conditions are independent of the particular closure assumptions used to model the Reynolds stresses, and the various forms are all equivalent in the limit $R_e \to \infty$. In the present study we have used the surface source formulation because it was best suited for matching to the strong interaction solutions and because it eliminates the need to modify the airfoil geometry in the solution procedure.

In this formulation the inviscid flow equations are solved subject to viscous boundary conditions on the airfoil and in wake given by:

$$V = \frac{1}{\rho_e} \frac{d\rho_e U_e \delta^*}{d S} \quad \text{on the airfoil surface } (N = 0) \tag{1}$$

$$\Delta V = \frac{1}{\rho_e} \frac{d\rho_e V_e \delta^*}{d S} \quad \text{on the wake streamline } (N = 0) \tag{2}$$

$$\Delta U = - U_e(\delta^*+\theta)\kappa \quad \text{on the wake streamline } (N = 0) \tag{3}$$

where V is velocity component normal to the airfoil surface, ΔV and ΔU are the jumps in the normal and tangential components of velocity across the wake streamline, ρ_e and U_e are the density and tangential velocity along the airfoil and wake, δ^* and θ are the displacement and momentum thicknesses of the shear layers, S and N are curvilinear coordinates along the normal to the streamline defining the airfoil and wake centerline, and κ is the curvature of the wake streamline. The three matching conditions can be formally derived from a standard asymptotic analysis in the limit $R_e \to \infty$.

Since the wake curvature condition is not as familiar as the other conditions we summarize the steps in its derivation. The condition arises from the pressure variation induced across the wake by the nonuniform velocity profile in the wake. A typical velocity profile and pressure variation in the wake are sketched in figure 2. In an inviscid flow the pressure gradient $\partial p/\partial N$ would be roughly constant across the wake and equal to

$$\left(\frac{\partial p}{\partial N}\right)_{\text{Inviscid}} = - \rho_e U_e^2 \kappa \tag{4}$$

In the viscous flow the pressure gradient is related to the actual velocity and density profiles in the wake $U(N,S)$, $\rho(N,S)$ by the normal momentum equation, as follows

$$\frac{\partial p}{\partial N} = - \rho(N,S)\, U^2(N,S)\kappa(S) \tag{5}$$

where it has been assumed that the streamlines in the wake are parallel, a justifiable assumption only in the part of the wake outside the trailing edge region. Subtraction of equations (4) and (5) followed by integration with respect to N and the imposition of the condition that the pressure in the viscous flow approach the linear variation implied by equation (4) as $N \to \pm \infty$ leads to the relation

$$\Delta P \equiv P^+ - P^- = - C_J(S)\kappa(S) \tag{6}$$

where

$$C_J = - \rho_e U_e^2 (\delta^* + \theta) \qquad < 0 \tag{7}$$

and P^+, P^- are the limiting values of the pressure in the outer inviscid flow on the upper and lower sides of the wake streamline, as indicated in figure 2. Equation (6) is similar to the boundary condition that arises in jet flap analysis, except that there C_J is the jet momentum coefficient which is a positive constant that is given as part of the data.

For small discontinuities, the pressure and velocity discontinuities are related by $\Delta P = - \rho_e U_e \Delta U$. Combining this expression with Equation (6) leads to the wake condition given in equation (3). In the present work we employ an irrotational approximation to the outer inviscid flow and the wake curvature condition is implemented by prescribing a jump in velocity potential, Γ, across the wake streamline, where

$$\Gamma \equiv \phi^+ - \phi^- \tag{8}$$

Since $\Delta U = d\Gamma/dS$ we arrive at the final condition used in the computation, namely

$$\frac{d\Gamma}{dS} = - U_e (\delta^* + \theta) \frac{d\beta}{dS} \tag{9}$$

where β is the angle the wake streamline makes with the chord of the airfoil. At a given stage of the numerical solution, the right side of equation (9) is known and Γ can be evaluated by simple quadrature.

TRAILING EDGE CORRECTIONS

The source velocity, V, streamline curvature, κ, and the velocity jump, ΔU, appearing in the matching conditions all develop square root singularities and become unbounded at the trailing edges of lifting airfoils (see ref. 7). As a result, the Kutta condition cannot be satisfied, the lift cannot be determined and the conventional boundary layer theory cannot strictly be used to determine the viscous flow over lifting airfoils. Existing methods employing boundary layer theory apparently circumvent these shortcomings by numerically smoothing the inviscid and boundary layer solutions near trailing edges and by iterating the coupled inviscid and boundary layer equations to obtain a self-consistent solution. The iteration seems to eliminate the singularities but is not consistent with an order of magnitude analysis of the normal momentum equation.

A completely consistent treatment of the flow near trailing edges was carried out by the author and his associates for airfoils with cusped trailing edges (see ref. 7). In that analysis we showed that normal pressure gradients across the boundary layer and wake are important and must be included in the lowest-order description of the local solution. We also showed that the flow near the trailing edge could be treated as an inviscid rotational flow, and we obtained complete analytic solutions of the relevant equations governing the leading terms of the local solution. Readers interested in this aspect of the problem should consult ref. 7 for further details.

In this section we indicate how the local trailing edge solution can be used to correct conventional boundary layer theory to obtain composite solutions that are uniformly valid near trailing edges. In our approach we represent the solution by standard composite expressions that are valid in the inviscid, boundary layer, wake and trailing edge regions. For example, the representations for the pressure coefficient C_p and normal velocity v are written in the form

$$C_p = \overbrace{C_{p,\text{outer}}(S,N;R_e)}^{\text{from the inviscid solution}} + \overbrace{[C_{p,\text{inner}}(S,N;R_e) - C_{p,\text{com}}(S,N;R_e)]}^{\Delta C_p} \tag{10}$$

$$v = \overbrace{v_{\text{outer}}(S,N;R_e)}^{\text{from the inviscid solution}} + [v_{\text{inner}}(S,N;R_e) - v_{\text{com}}(S,N;R_e)] \tag{11}$$

where v is velocity component along a curvilinear coordinate that is normal to the airfoil at the surface. The first terms on the right side of equations (10) and (11) are solutions of the outer inviscid flow equations that satisfy a set of corrected matching conditions. The second terms in equations (10) and (11) are from solutions to the inner shear layer equations valid near the airfoil and wake, including the strong interaction zone near the trailing edge. The last term with subscript "com" is the common part of the outer and inner solution and is determined as part of the inner solution. We should stress that the individual terms in the representation are not expanded in formal sum type asymptotic series in terms of the Reynolds number as in the usual method of matched asymptotic expansions. Instead, the inner and outer terms are determined from iterative solution of the coupled inviscid and shear layer equations.

If the standard boundary layer matching conditions were employed with the above representations, the above procedure would be equivalent to the conventional boundary layer type solution and would also break down near trailing edges. The key to our approach is to develop modified or "composite" matching conditions such that the above representation reduces to the usual boundary layer and inviscid solutions outside the trailing edge region and to the appropriate strong interaction solution near the trailing edge. The fact that this representation can be made to work is due to the close relationship between the downwash generated by the vorticity in the shear layers and the surface source velocities generated by the displacement thickness.

The appropriate correction to the matching conditions are generated as follows: First, the source velocities, V, on the upper and lower sides of the airfoil are linearly combined into symmetric and antisymmetric components defined by

$$V_A \equiv \frac{1}{2}(V^+ - V^-) \qquad V_S \equiv \frac{1}{2}(V^+ + V^-) \tag{12}$$

where V^+ and V^- are computed from equation (1) evaluated on the upper and lower sides of the airfoil, respectively. Then V_A and V_S are multiplied by corrections G_A and G_S

$$V_{A\ \text{corrected}} = V_A\, G_A \quad ; \quad V_{S\ \text{corrected}} = V_S\, G_S \tag{13}$$

where G_A and G_S are the ratios of the inner solution to its common part for the antisymmetric and symmetric components of the downwash velocity as determined from the inner solution. Next, equations (13) are recombined to form corrected expressions for the source velocities on the airfoil and wake as follows:

On the Airfoil:

$$V^+_{\text{corrected}} = V_{A,\ \text{corrected}} + V_{S,\ \text{corrected}} \tag{14a}$$

$$V^-_{\text{corrected}} = V_{A,\ \text{corrected}} - V_{S,\ \text{corrected}} \tag{14b}$$

In the Wake:

$$V_{\text{corrected}} = 2\, V_{S,\ \text{corrected}} \tag{14c}$$

A similar procedure is followed to correct the wake curvature term, leading to the expression

$$\frac{d\Gamma}{dS} = -\left[U_e(\rho^*+\theta)\frac{d\beta}{dS}\right] G_W \tag{14d}$$

where G_W is the ratio of the inner solution to its common part for the pressure jump across the wake streamline as determined from the trailing edge solution. Closed form expressions for the correction factors G_A, G_S, and G_W as determined from the local trailing edge solution are given in reference 7. All three functions approach one and the matching conditions reduce to conventional boundary layer forms outside the trailing edge interaction zone. Inside the interaction zone equations (14) reduce to forms that will recover the local trailing edge solution when combined with solutions of the outer inviscid equations.

The correction functions completely eliminate the singularities arising in the conventional matching conditions and lead to solutions that are uniformly valid in the trailing edge region. We also note that the matching conditions lead to discontinuities in the pressure across the wake in the outer inviscid

solution given by the first term in equation (10). A typical solution of the outer inviscid equations which shows the jump in pressure at the trailing edge is given in figure 3. Compensating discontinuities also arise in the second and third terms of equation (10), which exactly cancel the jump in the first term leading to a composite solution that is continuous across the wake, as it should be. Similar considerations also apply to the solution for the normal component of velocity. The airfoil is not a streamline of the outer inviscid flow since v_{outer} is not equal to zero on the airfoil surface, but is in fact, equal to a function determined by the corrected viscous matching conditions. However, the sum of the various terms on the right side of equations (11) all cancel at the airfoil surface with the result that v is equal to zero at the surface and the airfoil is a stream surface in the composite solution.

SOLUTION PROCEDURE

With the modified matching conditions discussed above the determinaton of the viscous flow over airfoils is reduced to the familar problem of solving the coupled inviscid and boundary layer equations. Solution to the inviscid equations are obtained with the relaxation techniques of BGKJ (ref. 3) for the full potential flow equation. We employed the particular version developed by Jameson (ref. 11) to provide a fully conservative, "rotated" scheme. An option is also provided to allow for a standard nonconservative formulation. The calculations are carried out in a computational plane obtained by conformally mapping the airfoil to a circle. The solution employs a sequence of meshes and uses Jameson's accelerated iterative method (ref. 11) to speed convergence.

The integral parameters appearing in the matching conditions are determined from solution of the boundary layer equations. The equations were solved with simple integral methods consisting of a compressible version of Thwaite's method for the laminar boundary layer near the leading edge and Green's lag-entrainment method (ref. 12) for the turbulent flow downstream of transition. The transition point locations can either be assigned or predicted by one of three standard semiempirical methods programmed into the code. Jump conditions are imposed across the transition point to define initial data for the turbulent calculation downstream of transition. Green's lag-entrainment equations are a set ordinary differential equations, which are solved by a standard Runge-Kutta method. The lag-entrainment equations include "history effects" through an approximate treatment of the turbulent energy equation. The wake is modeled in Green's method as independent symmetric half-wakes and seems to provide a reasonable engineering description of the integral parameters in the wake. The method is known to be about as accurate as Bradshaw's "TKE" finite difference method for airfoil type flows. We modified the original method to permit a reasonable treatment of flows with slender separation bubbles. As a result, the present computer code will function when separation occurs, but the accuracy of the method in this case is uncertain.

Solutions to Green's equations are discontinuous across shock waves. In order to obtain reasonable inputs for the subsequent inviscid solution the pressure distribution input to the boundary layer equations is smoothed over

a limited region near shock waves. Experience with the code indicates that the overall solution is insensitive to the degree of local smoothing applied in this way. Although the theory is strictly rational only for airfoils with cusped trailing edges the program can be applied to airfoils with finite trailing angles. Good results have been obtained for airfoils with included angles as large as 10°.

The iteration between the inviscid and viscid solutions is controlled by monitoring the maximum residual, which is a parameter that measures the degree of convergence of the inviscid solution. The boundary layer equations are solved and the matching conditions are updated whenever the maximum residual is reduced by a specified factor, typically equal to five.

All calculations were carried out on an IBM 370/168 computer. Typical runs for a full viscous solution required about five minutes to reduce the maximum residual to 10^{-5} on a 32 x 128 point grid.

RESULTS

In this section we report on results obtained with the new program. Comparisons of the theoretical results with wind tunnel data are presented for two airfoils, one a moderately rear loaded supercritical airfoil, the KORN I, which was tested at the National Aeronautical Establishment in Ottawa, and the other a newly designed NASA supercritical airfoil with large rear loading that was tested in the NASA Langley 8-foot transonic tunnel. Theoretical results are also presented which show the effect of neglecting the wake curvature term and of using a nonconservative formulation in the inviscid solution.

The test of the KORN I airfoil at Ottawa was carried out at a Reynolds number of 21.7×10^6 with the tunnel walls set at 20.5 percent porosity. Under these conditions blockage effects were small, but downwash effects due to the walls were large. Therefore, angle of attack corrections developed for the facility were applied to the data. (See reference 7 for further details.) The airfoil was aerodynamically smooth and was tested with natural transition. The calculations were carried out with transition fixed at 10% chord. This is a reasonable estimate considering the high Reynolds number of the test. The theoretical solutions were found to be relatively insensitive to the assumed position of the transition point.

The theoretical surface pressures are compared with experimental data in figure 4 for a free stream Mach number, $M = 0.699$ and an angle of attack $\alpha = 1.69°$ (corrected). The fully conservative solution and the experimental data are seen to be in good agreement. The agreement of the nonconservative solution with the data is much poorer. Since the drag coefficient of the nonconservative solution given in the figure does not include the mass flow correction that Garabedian (ref. 13) has shown to be necessary, the favorable agreement of the uncorrected drag result with data is fortuitous.

Comparisons of theory and experiment for the lift curve at M = 0.699 are given in figure 5. The results show that the viscous and wall interference effects are about the same magnitude. The results of the theory show very good agreement with corrected wind tunnel data. The choice of conservative or nonconservative differencing seems to have only a small effect on the solution for the lift coefficient. The present code was also used to obtain a conventional boundary layer solution by dropping the terms arising from the wake and the trailing edge correction terms. The computed result is labeled SCBL theory (self-consistent boundary layer theory) in the figure. This result indicates that conventional boundary layer predicts only about half the viscous loss of lift. This is more clearly brought out in the results plotted in figure 6.

In figure 6 we present results that illustrate the separate effects of wake curvature and trailing edge interaction on the lift coefficient. Four solutions, all obtained with the present code, are presented for the variation of lift coefficient with Mach number at a fixed incidence, $\alpha = 1.69°$, including the inviscid solution, the full viscous solution, the same solution with the wake curvature terms omitted, and the conventional self-consistent boundary layer solution (SCBL) mentioned above. The results in figure 6 clearly show that the conventional boundary layer approach underpredicts the boundary layer effect by about 50 percent. The difference between the self-consistent boundary layer solution and the viscous solution without wake curvature represents the effect of normal pressure gradients in the trailing edge region. The results in figure 6 indicate that this effect and the wake curvature effect combine to make up the other 50 percent of the lift reduction induced by the boundary layer. Thus the simple displacement surface type boundary layer formulation significantly underpredicts the boundary layer effect.

The drag polar for M = 0.699 is given in figure 7. Theoretical results for the full viscous theory using both the conservative and nonconservative formulation are compared with experimental data. A similar comparison presented in reference 7 was in error due to a mistake in the nonconservative solution. The conservative and nonconservative solutions are seen to differ significantly at the higher lift coefficients where shock waves are present in the solutions. Garabedian (ref. 13) has shown that the error in the nonconservative formulation is due to a spurious sink drag at the shock wave. The conservative solution leads to a reasonable prediction of the overall shape of the drag polar, but underestimates the drag levels by about 15 percent. There is some evidence (ref. 14) that experimental uncertainty in the drag measurements might be responsible for the poor agreement shown in this case.

Much better agreement is obtained with drag measurements from the 8-foot transonic wind tunnel at the NASA Langley Research Center. In figure 8 we present the results for the drag polar of the second airfoil considered in this paper. The airfoil is a 10 percent thick, heavily rear-loaded supercritical airfoil recently designed and tested at NASA Langley. Theoretical solutions with and without wake curvature are given in the figure together with a solution obtained with the nonconservative formulation. A blockage

correction of $\Delta M = -0.01$ was employed in the theoretical computations. Although, accurate wall corrections are not available for this facility recent studies, carried out at NASA Langley Research Center, have indicated that corrections of this magnitude are appropriate. Transition was fixed in the tests by placing transition strips at 28 percent chord and was fixed at the same location in the computations. The tests were carried out at a Reynolds number of $R_e = 7.7 \times 10^6$. The results in figure 8 show that the new viscous theory with wake curvature not only predicts the shape of the drag polar but also the absolute levels of drag over a wide range of lift coefficients. The results also show that the neglect of wake curvature leads to a noticeable underprediction of the drag and that the nonconservative formulation leads to a significant overestimate of the drag.

In figure 9 we compare the theoretical and experimental pressure distributions for a point about half way up the drag rise on the polar. The results show good agreement for both the pressure distribution and shock position. The slight underpredictions of the pressure over the rear upper surface were found to be due to numerical problems with code that have since been eliminated.

The solution for the lift curve is given in figure 10. The solutions clearly show the large effect of wake curvature on the predicted lift coefficient. The type of differencing is seen to have only a slight influence on the predicted lift coefficient. Uncorrected data from the test are also plotted in the figure for reference. The results are suggestive of relatively large wall induced downwash on the airfoil. However since accurate angle of attack corrections were not available comparisons with corrected data could not be provided.

CONCLUSIONS

The main conclusions to be drawn from the results obtained to date with the new viscous theory are:

- Wake curvature and trailing edge interaction effects are required in a completely consistent theory of viscous flow over airfoils. Together they account for about a half of the reduction of lift caused by the boundary layer. They are most important for rear loaded airfoils

- The new theory leads to accurate predictions of lift and drag provided a fully conservative differencing scheme is used to solve the equations. Both the shape of the drag polar and the absolute levels of the drag are well predicted by the theory.

The above are only tentative conclusions. The uncertainties in the drag measurements of the Ottawa facility and the unknown level of the angle of attack and blockage corrections required in the Langley tunnel prevent us from drawing more definite conclusions regarding the adequacy of the new theory. A more clear-cut validation of the theory would require improved wind tunnel tests with either small wall effects or accurate and documented corrections.

REFERENCES

1. Deiwert, G.S., "Computation of Separated Transonic Turbulent Flow," AIAA J., vol. 14, 1976.

2. Baldwin, B.S. and Lomax, H., "Thin Layer Approximation and Algebraic Model for Separated Turbulent Flow," AIAA Paper 78-257, 1978.

3. Bauer, F., Garabedian, P., Korn, D. and Jameson, A., Supercritical Wing Sections II," Springer-Verlag, New York, 1975.

4. Thwaites, B., Incompressible Aerodynamics, Oxford University Press, pp. 191-194, 1960.

5. Spence, D.A. and Beasley, J.A., "The Calculation of Lift Curve Slopes, Allowing for Boundary Layer, with Application to the RAE 101 and 104 Aerofoils," Rep. Memor. Aero. Res. Counc., London, 3137, 1960.

6. Lock, R.C., "Research in UK On Finite Difference Methods for Computing Steady Transonic Flows," Symposium Transsonicum II, Springer-Verlag, New York, 1975.

7. Melnik, R.E., Chow, R. and Mead, H.R., "Theory of Viscous Transonic Flow Over Airfoils at High Reynolds Numbers," AIAA Paper No. 77-680, 1977.

8. Melnik, R.E. and Grossman, B., "Further Developments in an Analysis of the Interaction of a Weak Normal Shock Wave with a Turbulent Boundary Layer," Symposium Transsonicum II, Springer-Verlag, 1975.

9. Melnik, R.W. and Chow, R., "Asymptotic Theory of Two Dimensional Trailing Edge Flows," NASA Conference on Aerodynamic Analysis Requiring Advanced Computors NASA SP 347, 1975 (also Grumman Research Department Report RE-510J).

10. Lighthill, M.J., "On Displacement Thickness," J. Fluid Mech., Vol. 4, 1958.

11. Jameson, A., "Numerical Computation of Transonic Flow with Shock Waves," Symposium Transsonicum II, Springer-Verlag, New York, 1975.

12. Green, J.E., Weeks, D.J., and Broomen, J.W.F., "Prediction of Turbulent Boundary Layers and Wakes in Compressible Flow by a Lag Entrainment Method," RAE Tech. Report, 72231, 1973.

13. Garabedian, P.R., "Transonic Flow Theory of Airfoils and Wings," Advances in Engineering Sciences, NASA CP-2001, 1976.

14. Ohman, L.H., Kacprzynski, J.H., and Brown, D., "Some Results from Tests in the NAE High Reynolds Number Two-Dimensional Test Facility on Shockless and other Airfoils," Canadian Aero. and Space Journ., Vol. 19, 1973.

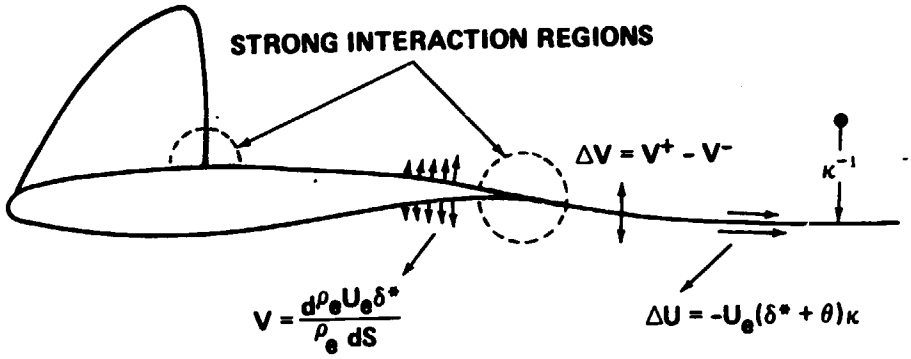

Figure 1.- Flow structure and viscous matching conditions.

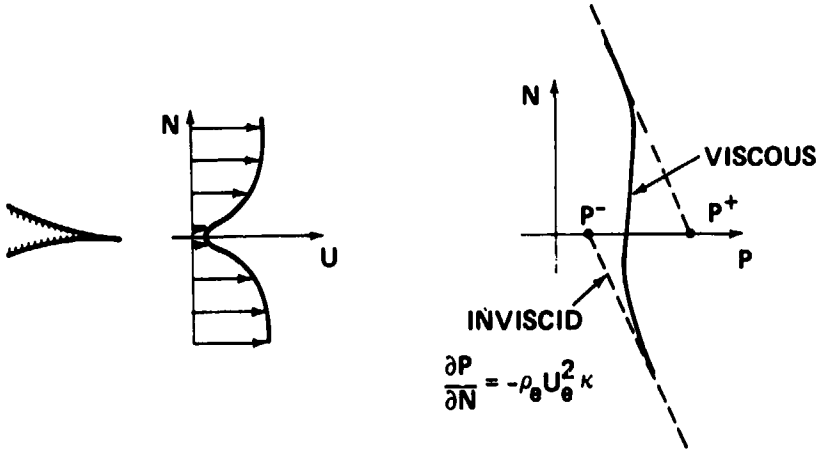

Figure 2.- Wake-curvature condition.

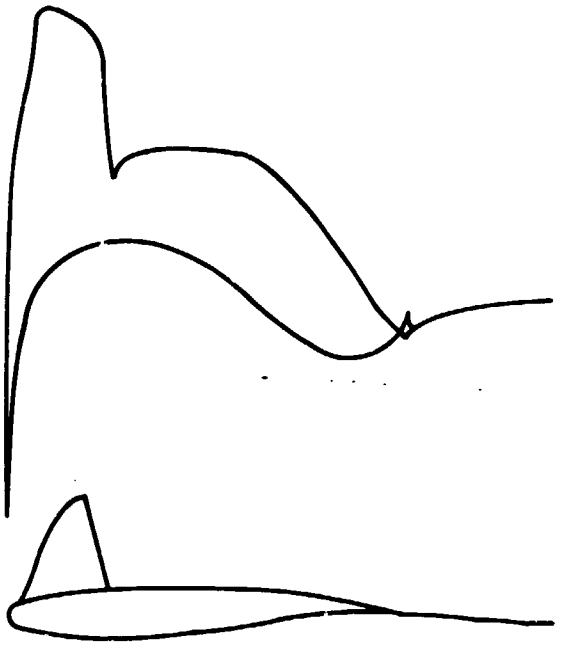

CL = .668 CD = .0082 CM = -.0989

Figure 3.- Outer inviscid solution for the pressure distribution where CL denotes lift coefficient, CD denotes drag coefficient, and CM denotes pitching-moment coefficient.

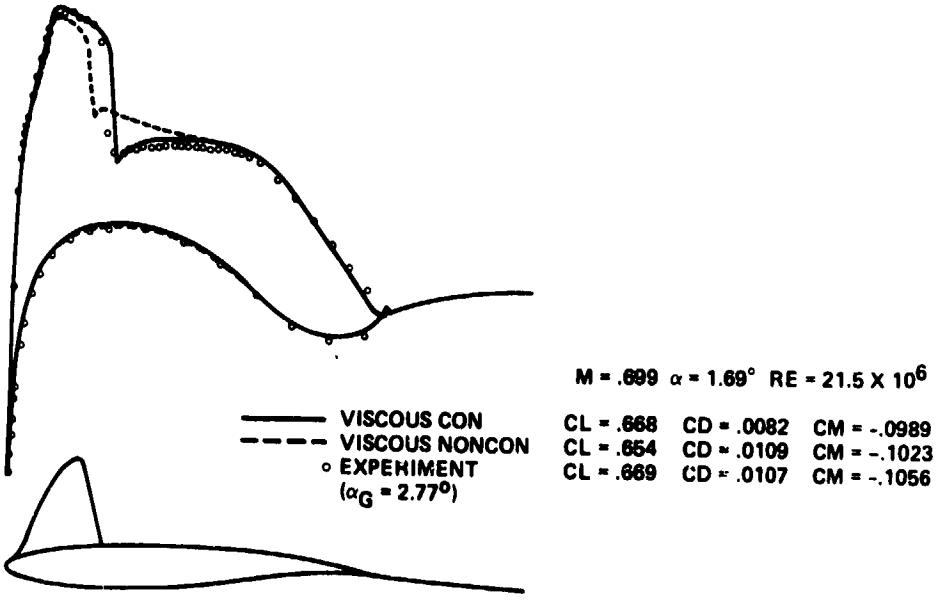

Figure 4.- Pressure distribution on a KORN I airfoil where RE denotes the Reynolds number.

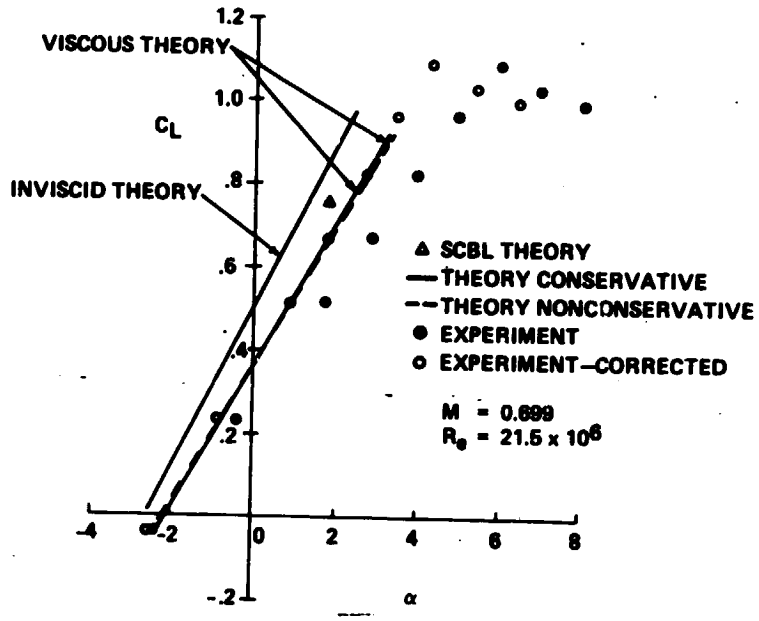

Figure 5.- Variation of lift coefficient with incidence for the KORN I airfoil.

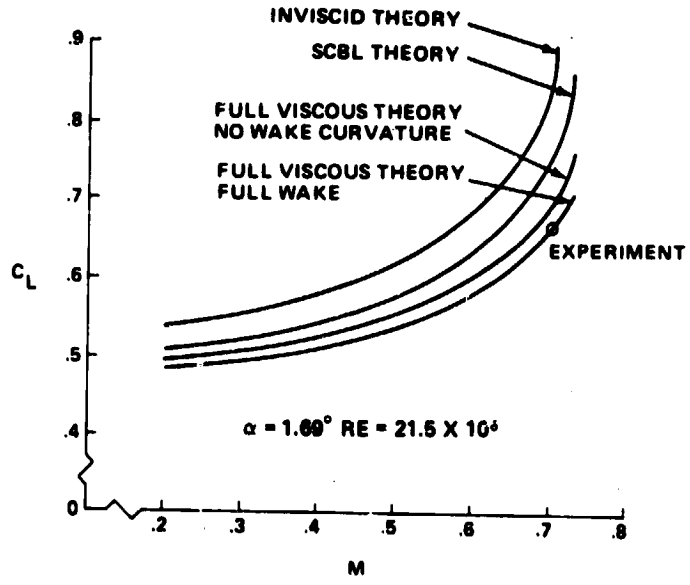

Figure 6.- Effect of wake curvature and strong interaction on lift.

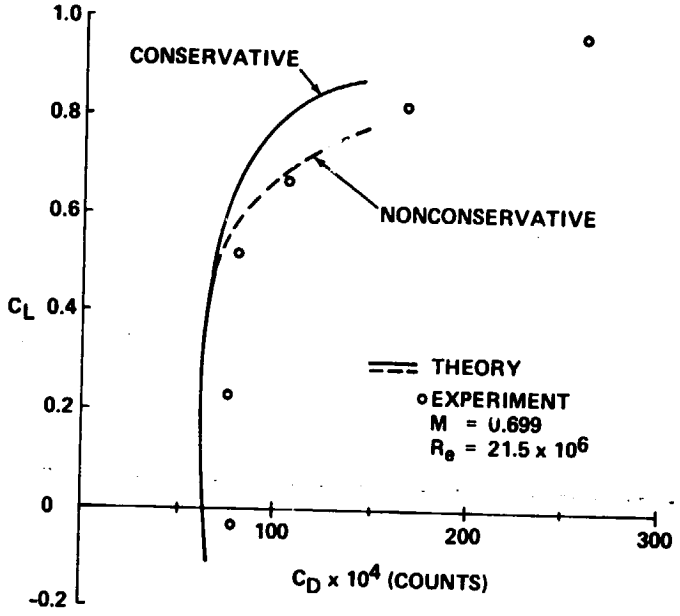

Figur- 7.- Drag polar for the KORN I airfoil.

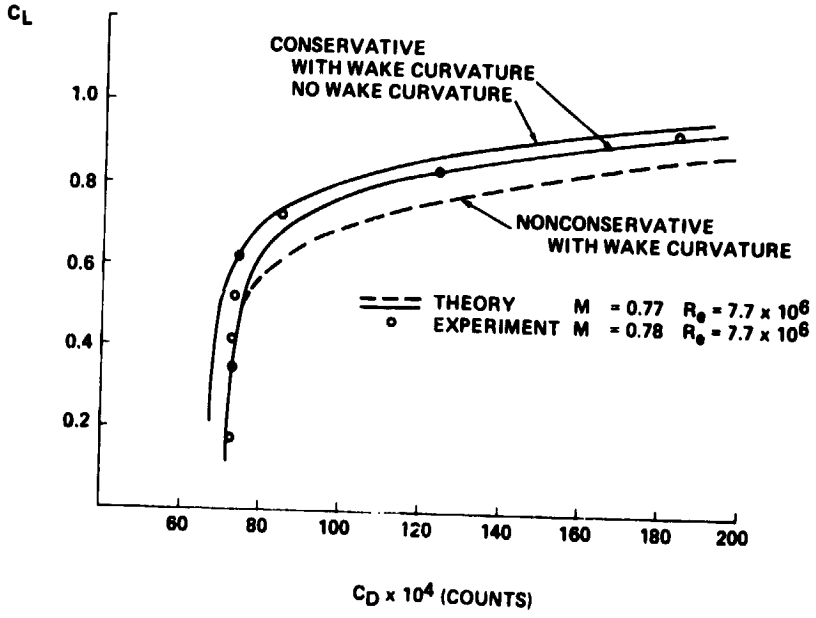

Figure 8.- Drag polar for the NASA supercritical airfoil.

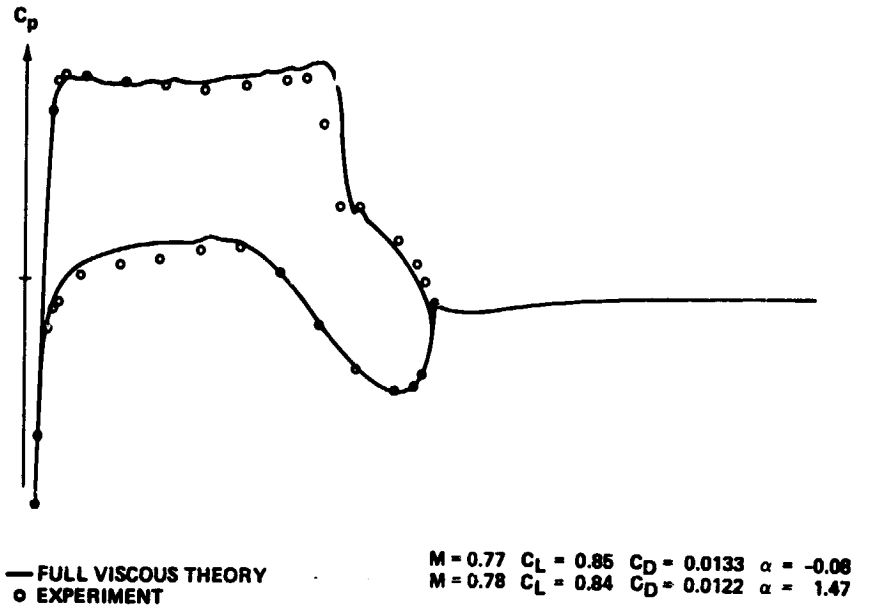

Figure 9.- Pressure distribution on the NASA airfoil.

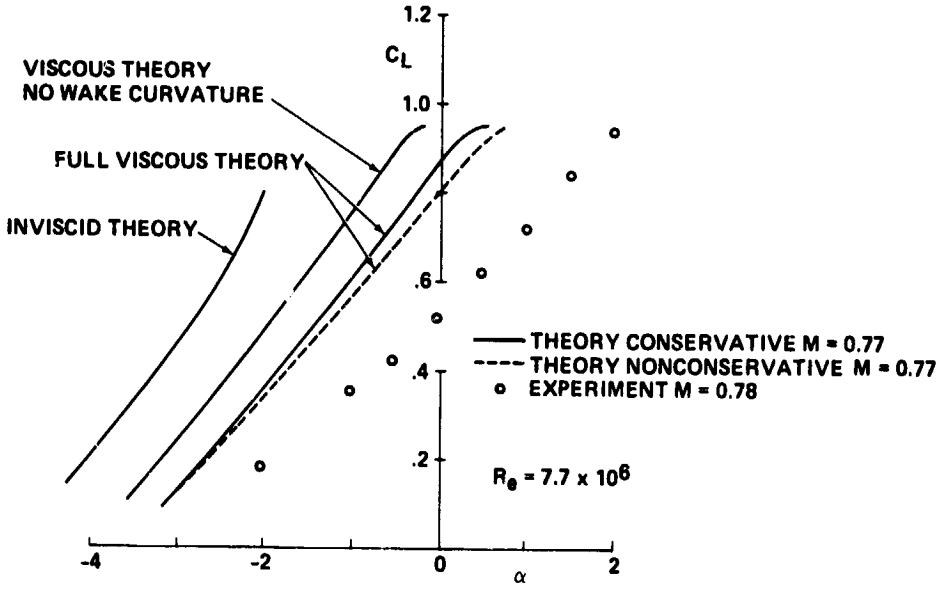

Figure 10.- Variation of lift coefficient with incidence for the NASA airfoil.